

The possibility to study in-medium modification of J/ψ mesons from their photoproduction on nuclei near threshold in the case of presence of the LHCb pentaquark states P_c^+ in this photoproduction

E. Ya. Paryev^{1,2}

¹*Institute for Nuclear Research, Russian Academy of Sciences,
Moscow 117312, Russia*

²*Institute for Theoretical and Experimental Physics,
Moscow 117218, Russia*

Abstract

We study the J/ψ photoproduction from nuclei in the near-threshold beam energy region of $E_\gamma=5-11$ GeV within the nuclear spectral function approach by considering incoherent direct ($\gamma N \rightarrow J/\psi N$) and two-step ($\gamma p \rightarrow P_c^+(4312)$, $P_c^+(4312) \rightarrow J/\psi p$; $\gamma p \rightarrow P_c^+(4440)$, $P_c^+(4440) \rightarrow J/\psi p$; $\gamma p \rightarrow P_c^+(4457)$, $P_c^+(4457) \rightarrow J/\psi p$) J/ψ production processes. We calculate the absolute excitation functions for the non-resonant and resonant production of J/ψ mesons off ^{12}C and ^{208}Pb target nuclei within the different scenarios for in-medium modification of the directly photoproduced J/ψ mesons and for branching ratios of the decays $P_c^+(4312) \rightarrow J/\psi p$, $P_c^+(4440) \rightarrow J/\psi p$ and $P_c^+(4457) \rightarrow J/\psi p$. We show that the non-resonant subthreshold J/ψ production in γA reactions reveals some sensitivity to employed in-medium modification scenarios for J/ψ mesons, which is not masked by the resonantly produced J/ψ mesons, only if above branching ratios are less than 5%. We also demonstrate that if these branching ratios more than 5% then the presence of the $P_c^+(4312)$, $P_c^+(4440)$ and $P_c^+(4457)$ resonances in J/ψ photoproduction on nuclei produces above threshold additional enhancements in the behavior of the total J/ψ creation cross section on nuclei, which could be also studied in the future JLab experiments at the CEBAF facility to provide both further evidence for their existence and valuable information on their nature.

1. Introduction

In a recent publication [1] the role of initially claimed [2] by the LHCb Collaboration pentaquark resonance $P_c^+(4450)$ in J/ψ photoproduction on nuclei at near-threshold incident photon energies of 5–11 GeV has been investigated within the spectral function approach. The description is based both on the direct non-resonant ($\gamma N \rightarrow J/\psi N$) and on the two-step resonant ($\gamma p \rightarrow P_c^+(4450)$, $P_c^+(4450) \rightarrow J/\psi p$) charmonium elementary production mechanisms. It was found that this role is not essential for the $P_c^+(4450)$ resonance with the spin-parity combination $J^P = (5/2)^+$ only if the branching fraction $Br[P_c^+(4450) \rightarrow J/\psi p] \sim 1\%$ and less. In this case the overall subthreshold J/ψ production in γA reactions reveals some sensitivity to adopted in-medium modification scenarios for the directly photoproduced J/ψ mesons.

Very recently, the LHCb Collaboration reported the observation of three new narrow pentaquark states [3]. Their updated analysis indicates that previously announced $P_c^+(4450)$ state splits into two narrow peaks, $P_c^+(4440)$ and $P_c^+(4457)$, in $J/\psi p$ invariant mass spectrum of the $\Lambda_b^0 \rightarrow K^-(J/\psi p)$ decays. Also a new pentaquark, $P_c^+(4312)$, was discovered in this spectrum. Since the current LHCb analysis [3] is not sensitive to broad resonances, it can neither confirm nor disprove the existence of the broad $P_c^+(4380)$ state observed in the original data [2]. The search for the LHCb pentaquark candidates $P_c^+(4312)$, $P_c^+(4440)$ and $P_c^+(4457)$ through a scan of the cross section of the exclusive reaction ¹⁾ $\gamma p \rightarrow J/\psi p$ from threshold of 8.2 GeV and up to photon energy $E_\gamma = 11.8$ GeV has been undertaken recently by the GlueX Collaboration at JLab [4]. No evidence for them has been found with present statistics and model-dependent upper limits on branching fractions of $P_c^+(4312) \rightarrow J/\psi p$, $P_c^+(4440) \rightarrow J/\psi p$ and $P_c^+(4457) \rightarrow J/\psi p$ decays were set. However, to get a robust enough information for or against their existence, improved separate P_c photoproduction measurements at JLab with finer energy binning and with using the polarization observables are needed (cf. [5, 6] and see also below).

Stimulated by the observation of the hidden-charm pentaquark resonances $P_c^+(4312)$, $P_c^+(4440)$ and $P_c^+(4457)$, we intend to investigate now their role in near-threshold J/ψ photoproduction off nuclei to shed light on the possibility to study experimentally the modification of the J/ψ meson mass in nuclear medium. The main purpose of the present paper is to extend the model [1] to J/ψ -producing two-step resonant processes $\gamma p \rightarrow P_c^+(4312)$, $P_c^+(4312) \rightarrow J/\psi p$; $\gamma p \rightarrow P_c^+(4440)$, $P_c^+(4440) \rightarrow J/\psi p$ and $\gamma p \rightarrow P_c^+(4457)$, $P_c^+(4457) \rightarrow J/\psi p$ as well as to incorporate in the calculations new experimental data for the total and differential cross sections of the $\gamma p \rightarrow J/\psi p$ reaction in the threshold energy region from the GlueX experiment [4]. Further, we briefly remind the main assumptions of the model [1] and describe, where it is necessary, the corresponding extensions. We present also the predictions obtained within this expanded model for the J/ψ excitation functions in γC and γPb collisions at near-threshold incident energies. These predictions can be used for possible extraction of valuable information on the J/ψ in-medium mass shift from the data which could be taken in a dedicated experiment at the upgraded up to 12 GeV CEBAF facility.

2. The framework

2.1. Direct mechanism of non-resonant J/ψ photoproduction on nuclei

At near-threshold photon beam energies below 11 GeV of our interest, the following direct non-resonant elementary J/ψ production processes contribute to the J/ψ photoproduction on nuclei [1]:

$$\gamma + p \rightarrow J/\psi + p, \quad (1)$$

¹⁾They should appear as structures at $E_\gamma = 9.44, 10.04$ and 10.12 GeV in this cross section.

$$\gamma + n \rightarrow J/\psi + n. \quad (2)$$

In line with [1], we approximate the in-medium local mass $m_{J/\psi}^*(\mathbf{r})$ of the J/ψ mesons, participating in the production processes (1), (2), with their average in-medium mass $\langle m_{J/\psi}^* \rangle$ defined as:

$$\langle m_{J/\psi}^* \rangle = m_{J/\psi} + V_0 \frac{\langle \rho_N \rangle}{\rho_0}. \quad (3)$$

Here, $m_{J/\psi}$ is the free space rest mass of a J/ψ meson, V_0 is its effective scalar potential (or its in-medium mass shift) at normal nuclear matter density ρ_0 , $\langle \rho_N \rangle$ is the average nucleon density. For target nuclei ^{12}C and ^{208}Pb , considered in [1] and here, the ratio $\langle \rho_N \rangle / \rho_0$ is approximately equal to 0.5 and 0.8, respectively. In what follows, in line with [1] for the J/ψ mass shift at normal nuclear matter density V_0 we will adopt the following options: i) $V_0 = 0$, ii) $V_0 = -25$ MeV, iii) $V_0 = -50$ MeV, iv) $V_0 = -100$ MeV, and v) $V_0 = -150$ MeV as well as will neglect the modification of the outgoing nucleon mass in nuclear matter.

Then, the total cross section for the production of J/ψ mesons on nuclei in the direct non-resonant processes (1) and (2) can be represented as follows [1]:

$$\sigma_{\gamma A \rightarrow J/\psi X}^{(\text{dir})}(E_\gamma) = I_V[A, \sigma_{J/\psi N}] \left\langle \sigma_{\gamma N \rightarrow J/\psi N}(E_\gamma) \right\rangle_A, \quad (4)$$

where the effective number of target nucleons participating in the primary $\gamma N \rightarrow J/\psi N$ processes, $I_V[A, \sigma_{J/\psi N}]$, and "in-medium" total cross section for the production of J/ψ with reduced mass $\langle m_{J/\psi}^* \rangle$ in reactions (1) and (2) $\sigma_{\gamma N \rightarrow J/\psi N}(\sqrt{s}, \langle m_{J/\psi}^* \rangle)$ at the γN center-of-mass energy \sqrt{s} , averaged over target nucleon binding and Fermi motion, $\left\langle \sigma_{\gamma N \rightarrow J/\psi N}(E_\gamma) \right\rangle_A$, are defined by Eqs. (5) and (6) in [1], respectively ²⁾. As in Ref. [1], for the J/ψ -nucleon absorption cross section $\sigma_{J/\psi N}$ we will use in our calculations the value $\sigma_{J/\psi N} = 3.5$ mb.

Also, as previously in [1], we suggest that the "in-medium" cross section $\sigma_{\gamma N \rightarrow J/\psi N}(\sqrt{s}, \langle m_{J/\psi}^* \rangle)$ for J/ψ production in processes (1) and (2) is equivalent to the vacuum cross section $\sigma_{\gamma N \rightarrow J/\psi N}(\sqrt{s}, m_{J/\psi})$ in which the free J/ψ mass $m_{J/\psi}$ is replaced by its average in-medium mass $\langle m_{J/\psi}^* \rangle$ as defined by equation (3) and the free space center-of-mass energy squared s , presented by the formula (9) below, is replaced by the in-medium expression

$$s = (E_\gamma + E_t)^2 - (\mathbf{p}_\gamma + \mathbf{p}_t)^2. \quad (5)$$

Here, E_γ and \mathbf{p}_γ are the energy and momentum of the incident photon, E_t and \mathbf{p}_t are the total energy and momentum of the struck target nucleons involved in the elementary processes (1) and (2). The quantity E_t is determined by Eq. (8) in Ref. [1]. For the free total cross section $\sigma_{\gamma N \rightarrow J/\psi N}(\sqrt{s}, m_{J/\psi})$ at photon energies $E_\gamma \leq 22$ GeV we have used the following expression, based on the near-threshold predictions of the two gluon and three gluon exchange model [7]:

$$\sigma_{\gamma N \rightarrow J/\psi N}(\sqrt{s}, m_{J/\psi}) = \sigma_{2g}(\sqrt{s}, m_{J/\psi}) + \sigma_{3g}(\sqrt{s}, m_{J/\psi}), \quad (6)$$

where

$$\sigma_{2g}(\sqrt{s}, m_{J/\psi}) = a_{2g}(1-x)^2 \left[\frac{e^{bt^+} - e^{bt^-}}{b} \right], \quad (7)$$

$$\sigma_{3g}(\sqrt{s}, m_{J/\psi}) = a_{3g}(1-x)^0 \left[\frac{e^{bt^+} - e^{bt^-}}{b} \right] \quad (8)$$

and

$$x = (s_{\text{thr}} - m_N^2)/(s - m_N^2); \quad s_{\text{thr}} = (m_{J/\psi} + m_N)^2, \quad s = (E_\gamma + m_N)^2 - \mathbf{p}_\gamma^2. \quad (9)$$

²⁾In equation (4) it is assumed, as previously in [1], that the J/ψ meson production cross sections in γp and γn interactions are the same.

Here, t^+ and t^- are the maximal and minimal values of the squared four-momentum transfer t between the incident photon and the outgoing J/ψ meson. They correspond to the t where the J/ψ is produced at angles of 0° and 180° in γp c.m.s., respectively, and can be expressed through the energies and momenta of the initial photon and the J/ψ meson, E_γ, p_γ and $E_{J/\psi}, p_{J/\psi}^*$, in this system in the following way:

$$t^\pm = m_{J/\psi}^2 - 2E_\gamma^*(m_N^2)E_{J/\psi}^*(m_{J/\psi}) \pm 2p_\gamma^*(m_N^2)p_{J/\psi}^*(m_{J/\psi}), \quad (10)$$

where

$$p_\gamma^*(m_N^2) = \frac{1}{2\sqrt{s}}\lambda(s, 0, m_N^2), \quad (11)$$

$$p_{J/\psi}^*(m_{J/\psi}) = \frac{1}{2\sqrt{s}}\lambda(s, m_{J/\psi}^2, m_N^2) \quad (12)$$

and

$$E_\gamma^*(m_N^2) = p_\gamma^*(m_N^2), \quad E_{J/\psi}^*(m_{J/\psi}) = \sqrt{m_{J/\psi}^2 + [p_{J/\psi}^*(m_{J/\psi})]^2}; \quad (13)$$

$$\lambda(x, y, z) = \sqrt{[x - (\sqrt{y} + \sqrt{z})^2][x - (\sqrt{y} - \sqrt{z})^2]}. \quad (14)$$

The elementary cross section (6)–(8) was used in the calculations of the non-resonant J/ψ pho-

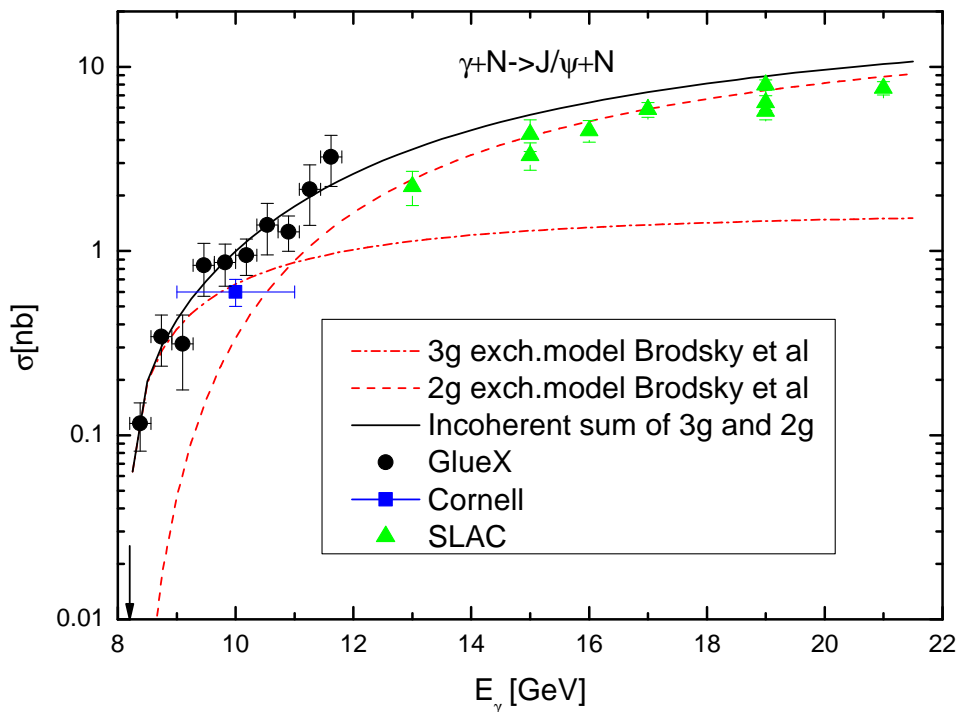


Figure 1: (color online) The non-resonant total cross section for the reaction $\gamma N \rightarrow J/\psi N$ as function of photon energy. Dashed and dotted-dashed curves: respectively, calculations on the basis of the two gluon and three gluon exchange model [7]. Solid curve: incoherent sum of the above two calculations. The GlueX and SLAC experimental data are from Ref. [4]. The Cornell data point is from Ref. [8]. The arrow indicates the threshold energy for direct J/ψ photoproduction on a free target nucleon being at rest.

toproduction off nuclei presented below. In this case the reaction $\gamma N \rightarrow J/\psi N$ goes in medium on an off-shell target nucleon. Then, according to above-mentioned, instead of the quantities m_N^2 and $m_{J/\psi}$, appearing in Eqs. (11) and (9), (12), (13), we should use the difference $E_t^2 - p_t^2$ and J/ψ average in-medium mass $\langle m_{J/\psi}^* \rangle$, respectively. And instead of the quantity s , appearing in Eqs. (9), (11), (12), one needs to adopt its in-medium expression (5). Parameter b in Eqs. (7), (8) is an exponential t -slope of the differential cross section of the reaction $\gamma p \rightarrow J/\psi p$ in the near-threshold energy region [7]. According to [4], $b \approx 1.67 \text{ GeV}^{-2}$. We will use this value in our calculations. The normalization coefficients a_{2g} and a_{3g} are determined assuming that incoherent sum (6) of both channels saturates the total experimental cross section of the reaction $\gamma p \rightarrow J/\psi p$ measured at GlueX [4] at photon energies around 8.38 and 11.62 GeV, at which the contribution of the pentaquark resonances $P_c^+(4312)$, $P_c^+(4440)$ and $P_c^+(4457)$ in J/ψ photoproduction on the proton is insignificant (see Fig. 2 given below). As a result, we get that $a_{2g} = 44.780 \text{ nb/GeV}^2$ and $a_{3g} = 2.816 \text{ nb/GeV}^2$. Fig. 1 shows that only the combination of the two gluon and three gluon exchange cross sections fits well the GlueX near-threshold data [4].

2.2. Two-step mechanism of resonant J/ψ photoproduction on nuclei

At photon energies below 11 GeV, an incident photon can produce a $P_c^+(4312)$, $P_c^+(4440)$ and $P_c^+(4457)$ resonances in the first inelastic collision with an intranuclear proton ³⁾:

$$\begin{aligned}\gamma + p &\rightarrow P_c^+(4312), \\ \gamma + p &\rightarrow P_c^+(4440), \\ \gamma + p &\rightarrow P_c^+(4457).\end{aligned}\tag{15}$$

Then the produced intermediate pentaquark resonances can decay into the J/ψ and p :

$$\begin{aligned}P_c^+(4312) &\rightarrow J/\psi + p, \\ P_c^+(4440) &\rightarrow J/\psi + p, \\ P_c^+(4457) &\rightarrow J/\psi + p.\end{aligned}\tag{16}$$

The branching ratios $Br[P_{ci}^+ \rightarrow J/\psi p]$ ⁴⁾ of these decays have not been determined yet. Model-dependent upper limits on these ratios of 4.6%, 2.3% and 3.8% for $P_c^+(4312)$, $P_c^+(4440)$ and $P_c^+(4457)$, assuming for each P_{ci}^+ spin-parity combination $J^P = (3/2)^-$, were set by the GlueX Collaboration [4]. They become a factor of 5 smaller if $J^P = (5/2)^+$ is supposed. Therefore, following Refs. [1, 4] as well as Refs. [5, 6, 9, 10], we will employ in our study for these three ratios three following main options: $Br[P_{ci}^+ \rightarrow J/\psi p] = 1, 2$ and 3% . To get a better impression of the size of the effect of branching fractions $Br[P_{ci}^+ \rightarrow J/\psi p]$ on the resonant J/ψ yield in $\gamma C \rightarrow J/\psi X$ and $\gamma \text{Pb} \rightarrow J/\psi X$ reactions, we will also calculate this yield additionally assuming that all these three branching fractions are equal to 5% [1] and 10% [5, 11].

According to [1], most of the $P_c^+(4312)$, $P_c^+(4440)$ and $P_c^+(4457)$ resonances, having vacuum total decay widths in their rest frames $\Gamma_{c1} = 9.8 \text{ MeV}$, $\Gamma_{c2} = 20.6 \text{ MeV}$ and $\Gamma_{c3} = 6.4 \text{ MeV}$ [3], respectively, decay to J/ψ and p outside the target nuclei considered. As in [1], their free spectral functions are described by the non-relativistic Breit-Wigner distributions:

$$S_{ci}(\sqrt{s}, \Gamma_{ci}) = \frac{1}{2\pi} \frac{\Gamma_{ci}}{(\sqrt{s} - M_{ci})^2 + \Gamma_{ci}^2/4}, \quad i = 1, 2, 3;\tag{17}$$

³⁾Let us remind that the threshold (resonant) energies E_γ^{R1} , E_γ^{R2} and E_γ^{R3} for the photoproduction of these resonances with pole masses $M_{c1} = 4311.9 \text{ MeV}$, $M_{c2} = 4440.3 \text{ MeV}$ and $M_{c3} = 4457.3 \text{ MeV}$ on a free target proton being at rest are $E_\gamma^{\text{R1}} = 9.44 \text{ GeV}$, $E_\gamma^{\text{R2}} = 10.04 \text{ GeV}$ and $E_\gamma^{\text{R3}} = 10.12 \text{ GeV}$, respectively.

⁴⁾Here, $i = 1, 2, 3$ and P_{c1}^+ , P_{c2}^+ , P_{c3}^+ stand for $P_c^+(4312)$, $P_c^+(4440)$, $P_c^+(4457)$, respectively.

where \sqrt{s} is the total γp center-of-mass energy given by Eq. (9)⁵⁾ and S_{c1}, S_{c2}, S_{c3} correspond to the $P_c^+(4312), P_c^+(4440)$ and $P_c^+(4457)$, respectively. Following [1], we assume that the in-medium $P_c^+(4312), P_c^+(4440)$ and $P_c^+(4457)$ resonances spectral functions $S_{c1}(\sqrt{s}, \Gamma_{\text{med}}^{c1}), S_{c2}(\sqrt{s}, \Gamma_{\text{med}}^{c2})$ and $S_{c3}(\sqrt{s}, \Gamma_{\text{med}}^{c3})$ are also described by the Breit-Wigner formula (17), respectively, with a total in-medium widths $\Gamma_{\text{med}}^{c1}, \Gamma_{\text{med}}^{c2}$ and Γ_{med}^{c3} in their rest frames, obtained as a sum of the vacuum decay widths, $\Gamma_{c1}, \Gamma_{c2}, \Gamma_{c3}$, and an in-medium contributions due to $P_{ci}^+ N$ inelastic collisions – averaged over local nucleon density $\rho_N(\mathbf{r})$ collisional widths $\langle \Gamma_{\text{coll},c1} \rangle, \langle \Gamma_{\text{coll},c2} \rangle$ and $\langle \Gamma_{\text{coll},c3} \rangle$:

$$\Gamma_{\text{med}}^{ci} = \Gamma_{ci} + \langle \Gamma_{\text{coll},ci} \rangle, \quad i = 1, 2, 3; \quad (18)$$

where, according to [1], the average collisional width $\langle \Gamma_{\text{coll},ci} \rangle$ reads:

$$\langle \Gamma_{\text{coll},ci} \rangle = \gamma_c v_c \sigma_{P_{ci}N} \langle \rho_N \rangle. \quad (19)$$

Here, $\sigma_{P_{ci}N}$ is the P_{ci}^+ -nucleon inelastic cross section⁶⁾ and the Lorentz γ -factor γ_c and the velocity v_c of the resonance P_{ci}^+ in the nuclear rest frame are given by formula (16) in [1].

Exploring the molecular scenario of $P_c^+(4312), P_c^+(4440)$ and $P_c^+(4457)$ states⁷⁾, in which their spins-parities are $J^P = (1/2)^-$ for $P_c^+(4312)$, $J^P = (1/2)^-$ for $P_c^+(4440)$ and $J^P = (3/2)^-$ for $P_c^+(4457)$ [5, 10, 13, 14], we can describe the free Breit-Wigner total cross sections for their production in reactions (15) on the basis of the spectral functions (17), provided that the branching ratios $Br[P_{ci}^+ \rightarrow \gamma p]$ are known, as follows [9, 11]:

$$\sigma_{\gamma p \rightarrow P_{ci}^+}(\sqrt{s}, \Gamma_{ci}) = f_{ci} \left(\frac{\pi}{p_\gamma^*} \right)^2 Br[P_{ci}^+ \rightarrow \gamma p] S_{ci}(\sqrt{s}, \Gamma_{ci}) \Gamma_{ci}, \quad i = 1, 2, 3; \quad (20)$$

where the center-of-mass momentum in the initial γp channel, p_γ^* , is defined above by Eq. (11) and the ratios of spin factors $f_{c1} = 1, f_{c2} = 1, f_{c3} = 2$.

Following [6, 11, 25], we assume that the $P_c^+(4312) (1/2)^-, P_c^+(4440) (1/2)^-$ and $P_c^+(4457) (3/2)^-$ decays to $J/\psi p$ are dominated by the lowest partial waves with relative orbital angular momentum $L = 0$. In this case the branching ratios $Br[P_c^+(4312) \rightarrow \gamma p], Br[P_c^+(4440) \rightarrow \gamma p]$ and $Br[P_c^+(4457) \rightarrow \gamma p]$ can be expressed using the vector-meson dominance model, respectively, via the branching fractions $Br[P_c^+(4312) \rightarrow J/\psi p], Br[P_c^+(4440) \rightarrow J/\psi p]$ and $Br[P_c^+(4457) \rightarrow J/\psi p]$ as follows [6, 9, 11, 25]:

$$Br[P_{ci}^+ \rightarrow \gamma p] = 4\pi\alpha \left(\frac{f_{J/\psi}}{m_{J/\psi}} \right)^2 f_{0,ci} \left(\frac{p_{\gamma,ci}^*}{p_{J/\psi,ci}^*} \right) Br[P_{ci}^+ \rightarrow J/\psi p], \quad i = 1, 2, 3; \quad (21)$$

where $f_{J/\psi} = 280$ MeV is the J/ψ decay constant, $\alpha = 1/137$ is the electromagnetic fine structure constant and

$$p_{\gamma,ci}^* = \frac{1}{2M_{ci}} \lambda(M_{ci}^2, 0, m_N^2), \quad p_{J/\psi,ci}^* = \frac{1}{2M_{ci}} \lambda(M_{ci}^2, m_{J/\psi}^2, m_N^2), \quad (22)$$

$$f_{0,ci} = \frac{2}{2 + \gamma_{ci}^2}, \quad \gamma_{ci}^2 = 1 + p_{J/\psi,ci}^{*2} / m_{J/\psi}^2. \quad (23)$$

⁵⁾When calculating the excitation functions for resonant production of $P_c^+(4312), P_c^+(4440)$ and $P_c^+(4457)$ states in reactions (15) on ^{12}C and ^{208}Pb targets in the "free" $P_c^+(4312), P_c^+(4440)$ and $P_c^+(4457)$ spectral function scenario (see Fig. 4 below), this energy is determined in line with Eq. (5).

⁶⁾We use in the following calculations $\sigma_{P_{ci}N} = 33.5$ mb [1] for each $i = 1, 2, 3$.

⁷⁾In this scenario, due to the closeness of the observed $P_c^+(4312)$ and $P_c^+(4440), P_c^+(4457)$ masses to the $\Sigma_c^+ \bar{D}^0$ and $\Sigma_c^+ \bar{D}^{*0}$ thresholds of 4317.7 and 4459.9 MeV [12], respectively, the $P_c^+(4312)$ resonance can be, in particular, considered as S-wave $\Sigma_c^+ \bar{D}^0$ bound state, while the $P_c^+(4440)$ and $P_c^+(4457)$ as S-wave $\Sigma_c^+ \bar{D}^{*0}$ bound molecular states [5, 10, 13–24].

Accounting for that $(p_{\gamma,c1}^*, p_{J/\psi,c1}^*, f_{0,c1}) = (2.054 \text{ GeV}/c, 0.658 \text{ GeV}/c, 0.657)$, $(p_{\gamma,c2}^*, p_{J/\psi,c2}^*, f_{0,c2}) = (2.121 \text{ GeV}/c, 0.810 \text{ GeV}/c, 0.652)$ and $(p_{\gamma,c3}^*, p_{J/\psi,c3}^*, f_{0,c3}) = (2.130 \text{ GeV}/c, 0.828 \text{ GeV}/c, 0.651)$, we get from Eq. (21):

$$\begin{aligned} Br[P_c^+(4312) \rightarrow \gamma p] &= 1.52 \cdot 10^{-3} Br[P_c^+(4312) \rightarrow J/\psi p], \\ Br[P_c^+(4440) \rightarrow \gamma p] &= 1.26 \cdot 10^{-3} Br[P_c^+(4440) \rightarrow J/\psi p], \\ Br[P_c^+(4457) \rightarrow \gamma p] &= 1.24 \cdot 10^{-3} Br[P_c^+(4457) \rightarrow J/\psi p]. \end{aligned} \quad (24)$$

The free resonant total cross sections $\sigma_{\gamma p \rightarrow P_{ci}^+ \rightarrow J/\psi p}(\sqrt{s}, \Gamma_{ci})$ for J/ψ production in the two-step processes (15), (16) can be represented as follows [1]:

$$\sigma_{\gamma p \rightarrow P_{ci}^+ \rightarrow J/\psi p}(\sqrt{s}, \Gamma_{ci}) = \sigma_{\gamma p \rightarrow P_{ci}^+}(\sqrt{s}, \Gamma_{ci}) \theta[\sqrt{s} - (m_{J/\psi} + m_N)] Br[P_{ci}^+ \rightarrow J/\psi p], \quad i = 1, 2, 3. \quad (25)$$

According to Eqs. (20) and (21) these cross sections are proportional to $Br^2[P_{ci}^+ \rightarrow J/\psi p]$.

In line with [1], we get the following expression for the J/ψ total cross section for γA reactions from the production/decay chains (15), (16):

$$\sigma_{\gamma A \rightarrow J/\psi X}^{(\text{sec})}(E_\gamma) = \sum_{i=1}^3 \sigma_{\gamma A \rightarrow P_{ci}^+ \rightarrow J/\psi p}^{(\text{sec})}(E_\gamma), \quad (26)$$

where

$$\sigma_{\gamma A \rightarrow P_{ci}^+ \rightarrow J/\psi p}^{(\text{sec})}(E_\gamma) = \left(\frac{Z}{A}\right) I_V[A, \sigma_{P_{ci}N}^{\text{eff}}] \left\langle \sigma_{\gamma p \rightarrow P_{ci}^+}(E_\gamma) \right\rangle_A Br[P_{ci}^+ \rightarrow J/\psi p] \quad (27)$$

and the quantities $I_V[A, \sigma_{P_{ci}N}^{\text{eff}}]$, $\left\langle \sigma_{\gamma p \rightarrow P_{ci}^+}(E_\gamma) \right\rangle_A$ are defined, respectively, by Eqs. (5), (24) of Ref. [1]. Here, $\sigma_{P_{ci}N}^{\text{eff}}$ is the P_{ci}^+ -nucleon effective absorption cross section. This cross section can be represented as follows [1]:

$$\sigma_{P_{ci}N}^{\text{eff}} = \sigma_{P_{ci}N} + \sigma_{\text{dec}}^{ci}, \quad i = 1, 2, 3; \quad (28)$$

where σ_{dec}^{ci} is the additional to the inelastic cross section $\sigma_{P_{ci}N}$ effective P_{ci}^+ absorption cross section associated with their decays in the nucleus. Using $\Gamma_{c1} = 9.8 \text{ MeV}$, $\Gamma_{c2} = 20.6 \text{ MeV}$ and $\Gamma_{c3} = 6.4 \text{ MeV}$, we obtain in the low-density approximation (19) that $\sigma_{\text{dec}}^{c1} = 2.83 \text{ mb}$, $\sigma_{\text{dec}}^{c2} = 5.75 \text{ mb}$ and $\sigma_{\text{dec}}^{c3} = 1.78 \text{ mb}$ for target nuclei considered in the case of the free P_{c1}^+ , P_{c2}^+ and P_{c3}^+ states production on a target proton at rest by incident photons with resonant energies $E_\gamma^{\text{R1}} = 9.44 \text{ GeV}$, $E_\gamma^{\text{R2}} = 10.04 \text{ GeV}$ and $E_\gamma^{\text{R3}} = 10.12 \text{ GeV}$. For numerical simplicity, we will employ in our calculations of the cross sections of (26), (27) for the quantity $\sigma_{P_{ci}N}^{\text{eff}}$ its average value $\sum_{i=1}^3 \sigma_{P_{ci}N}^{\text{eff}}/3$, which, according to Eq. (28) and with $\sigma_{P_{ci}N} = 33.5 \text{ mb}$, is approximately equal to 37 mb .

3. Results and discussion

The free elementary non-resonant J/ψ production cross section (6) (solid curve) and the combined (non-resonant plus resonant (25)) total cross sections (dashed, dotted and dotted-dashed curves) in comparison with the available low-energy experimental data are presented in Fig. 2. From this figure, one can see that the $P_c^+(4312)$ state appears as clear narrow independent peak at $E_\gamma = 9.44 \text{ GeV}$ in the combined cross section, while the $P_c^+(4440)$ and $P_c^+(4457)$ resonances exhibit itself here as such two distinct narrow overlapping peaks at $E_\gamma = 10.04$ and 10.12 GeV ⁸⁾, if $Br[P_{ci}^+ \rightarrow J/\psi p] = 3\%$ ($i = 1, 2, 3$). The strengths of these three peaks, obtained for $Br[P_{ci}^+ \rightarrow J/\psi p] \sim 1\text{--}2\%$, decrease essentially compared to the above case and have a peak values, which are compatible with the respective GlueX data points. To see experimentally such structures in the

⁸⁾With the distance between their centroids $\Delta E_\gamma = 80 \text{ MeV}$.

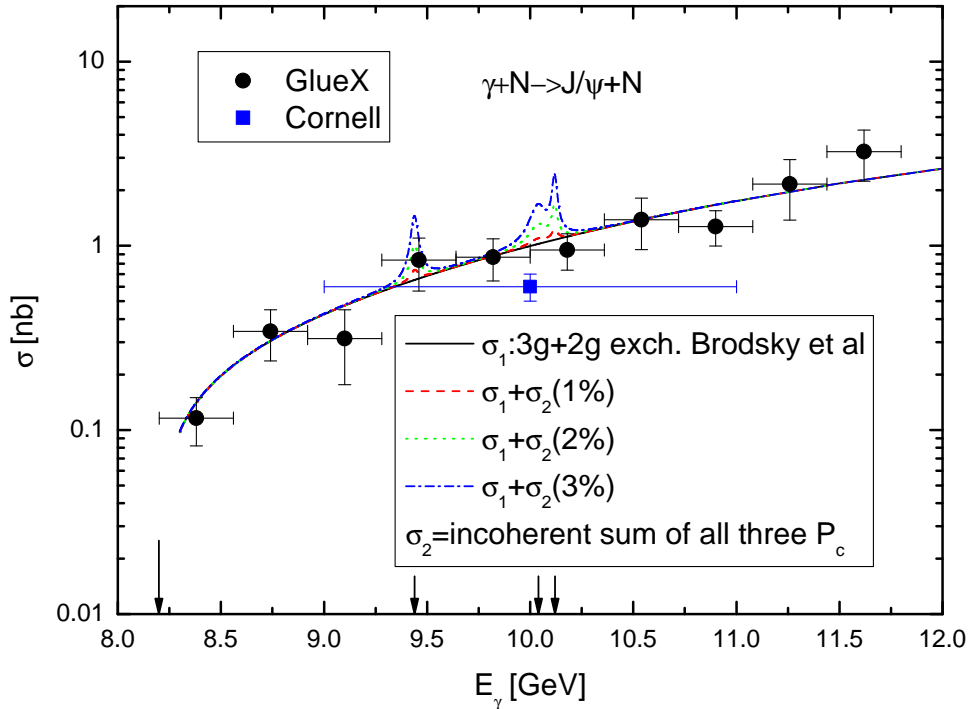


Figure 2: (color online) The non-resonant total cross section for the reaction $\gamma N \rightarrow J/\psi N$ (solid curve) and the incoherent sum of it and the total cross section for the resonant J/ψ production in the processes $\gamma p \rightarrow P_c^+(4312) \rightarrow J/\psi p$, $\gamma p \rightarrow P_c^+(4440) \rightarrow J/\psi p$ and $\gamma p \rightarrow P_c^+(4457) \rightarrow J/\psi p$, calculated assuming that the resonances $P_c^+(4312)$, $P_c^+(4440)$ and $P_c^+(4457)$ with the spin-parity quantum numbers $J^P = (1/2)^-$, $J^P = (1/2)^-$ and $J^P = (3/2)^-$ decay to $J/\psi p$ with the lower allowed relative orbital angular momentum $L = 0$ with all three branching fractions $Br[P_{ci}^+ \rightarrow J/\psi p] = 1$, 2 and 3% (respectively, dashed, dotted and dotted-dashed curves), as functions of photon energy. The left and three right arrows indicate, correspondingly, the threshold energy $E_\gamma^{\text{thr}} = 8.2$ GeV for the reaction $\gamma N \rightarrow J/\psi N$ proceeding on a free target nucleon being at rest and the resonant energies $E_\gamma^{\text{R1}} = 9.44$ GeV, $E_\gamma^{\text{R2}} = 10.04$ GeV and $E_\gamma^{\text{R3}} = 10.12$ GeV. The GlueX experimental data are from Ref. [4]. The Cornell data point is from Ref. [8].

combined total cross section of the reaction $\gamma p \rightarrow J/\psi p$ one needs to have a substantially finer energy binning than that of 360 MeV adopted in the GlueX experiment [4]. Thus, the c.m. energy ranges $M_{ci} - \Gamma_{ci}/2 < \sqrt{s} < M_{ci} + \Gamma_{ci}/2$ ($i = 1, 2, 3$) correspond to laboratory photon energy regions of $9.416 \text{ GeV} < E_\gamma < 9.461 \text{ GeV}$, $9.989 \text{ GeV} < E_\gamma < 10.086 \text{ GeV}$ and $10.103 \text{ GeV} < E_\gamma < 10.133 \text{ GeV}$, i.e. $\Delta E_\gamma = 45, 97$ and 30 MeV, for $P_c^+(4312)$, $P_c^+(4440)$ and $P_c^+(4457)$, respectively. This means that to resolve the three peaks in Fig. 2 the photon energy resolution and the energy bin size much less than at least 30 MeV are required⁹⁾. Otherwise, to compare correctly theoretical cross sections with the data of Fig. 2 it is necessary to smear the contributions from the resonant

⁹⁾At GlueX, the E_γ resolution amounts presently to 20 MeV for a 10 GeV photon [4]. Over time, it is expected to be around 6 MeV [11]. This translates into an uncertainty in c.m. energy of 1 MeV for a 10 GeV photon [11]. With such resolution (and bin size) will be possible to perform a detailed scan of the J/ψ total photoproduction cross section on a proton target in the near-threshold energy region around energies $E_\gamma = 9.44, 10.04$ and 10.12 GeV to obtain a definite result for or against the existence of the genuine $P_c^+(4312)$, $P_c^+(4440)$ and $P_c^+(4457)$ pentaquark states and to clarify their nature and decay probabilities (cf. [26]).

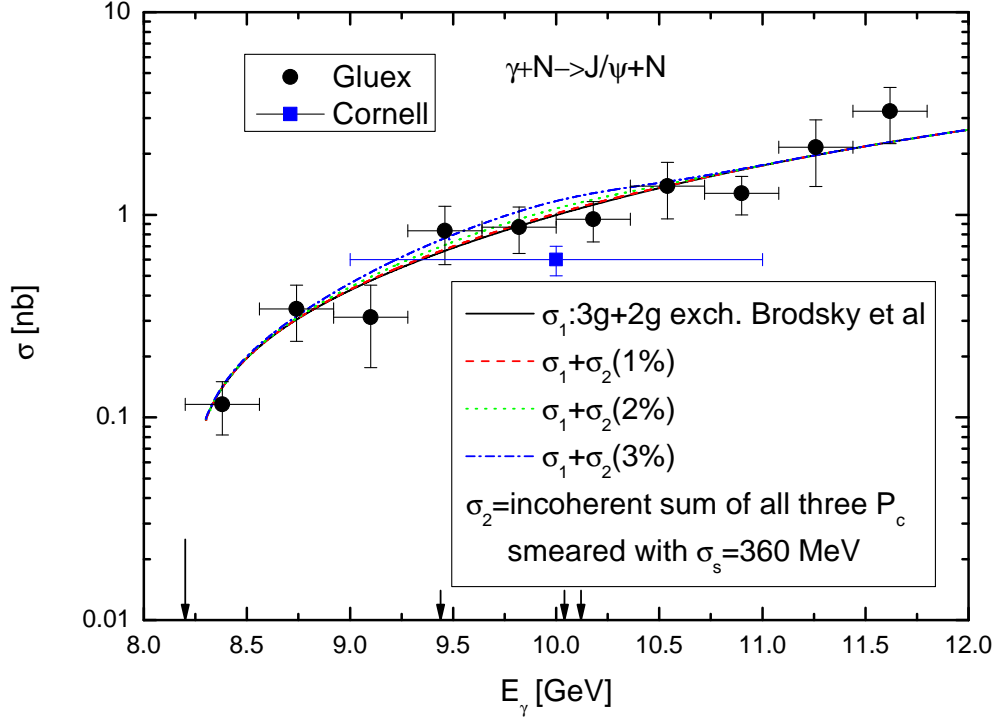


Figure 3: (color online) The same as in figure 2, but the contributions from the resonant channels $\gamma p \rightarrow P_c^+(4312) \rightarrow J/\psi p$, $\gamma p \rightarrow P_c^+(4440) \rightarrow J/\psi p$ and $\gamma p \rightarrow P_c^+(4457) \rightarrow J/\psi p$ are smeared by convoluting their with a Gaussian distribution as described in the text.

channels $\gamma p \rightarrow P_c^+(4312) \rightarrow J/\psi p$, $\gamma p \rightarrow P_c^+(4440) \rightarrow J/\psi p$ and $\gamma p \rightarrow P_c^+(4457) \rightarrow J/\psi p$ by convoluting their with a Gaussian distribution

$$G(x) = \frac{\exp(-x^2/2\sigma_s^2)}{\sqrt{2\pi}\sigma_s} \quad (29)$$

according to the expression [25]

$$\left\langle \sigma_{\gamma p \rightarrow P_{ci}^+ \rightarrow J/\psi p}(E_\gamma, \Gamma_{ci}) \right\rangle_s = \int_{-\infty}^{+\infty} \sigma_{\gamma p \rightarrow P_{ci}^+ \rightarrow J/\psi p}(\sqrt{s}(E_\gamma = y), \Gamma_{ci}) G(E_\gamma - y) dy, \quad i = 1, 2, 3; \quad (30)$$

where σ_s is the parameter of smearing. Since in the GlueX experiment the E_γ bin size is much larger than the E_γ resolution, we use in smearing (30) for this parameter the value of the bin size, i.e. $\sigma_s = 360$ MeV. The results of such smearing of the resonant contributions in J/ψ production on proton target are given in Fig. 3. It is seen that the peak structures of Fig. 2, corresponding to the $P_c^+(4312)$, $P_c^+(4440)$ and $P_c^+(4457)$ states, disappear now. The resulting combined total cross sections lie inside the experimental errors, which do not allow to distinguish between adopted three realistic options for branching fractions $Br[P_{ci}^+ \rightarrow J/\psi p]$, and their shapes agree well with GlueX measurements. It is worth noting that three-peak structure of Fig. 2, corresponding to the case of no smearing, is also seen, as showed our calculations, when the smearing parameter $\sigma_s = 20$ MeV is used in Eq. (30). Now, the strengths of the peaks decrease slightly and become slightly broader compared to those of Fig. 2. This indicates that indeed to observe the signals from the pentaquark

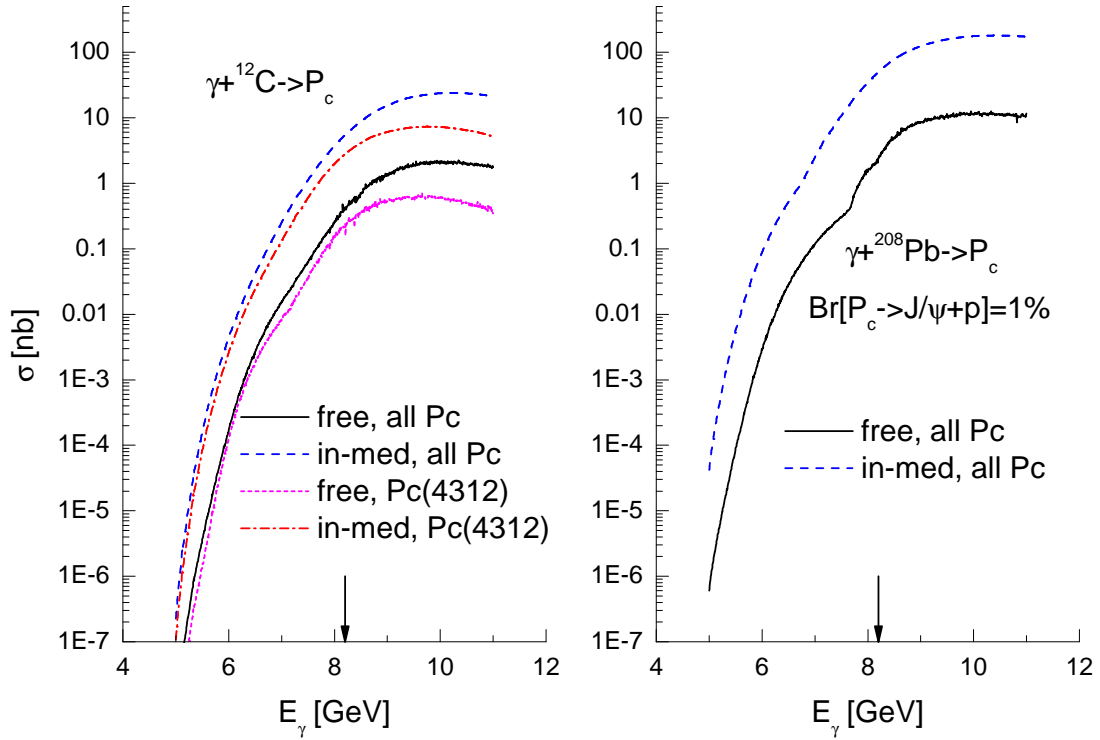


Figure 4: (color online) Excitation functions for resonant production of $P_c^+(4312)$, $P_c^+(4440)$ and $P_c^+(4457)$ states off ^{12}C and ^{208}Pb from the processes $\gamma p \rightarrow P_c^+(4312)$, $\gamma p \rightarrow P_c^+(4440)$ and $\gamma p \rightarrow P_c^+(4457)$ going on an off-shell target protons, calculated for $Br[P_{ci}^+ \rightarrow J/\psi p] = 1\%$ for all i adopting free (solid curves) and in-medium (dashed curves) P_{ci}^+ spectral functions. ^{12}C case: the same as above, but only for the process $\gamma p \rightarrow P_c^+(4312)$, employing free (short-dashed) and in-medium (dotted-dashed) $P_c^+(4312)$ spectral functions. The arrows indicate the threshold energy for direct J/ψ photoproduction on a free target nucleon being at rest.

states P_{ci}^+ one should choose the energy bin size \sim a few tens MeV (and determine the photon energy with precision higher than this size).

Figure 4 shows the energy dependences of the total $P_c^+(4312)$, $P_c^+(4440)$ and $P_c^+(4457)$ production cross section in γC and γPb reactions as well as of the total $P_c^+(4312)$ creation in γC collisions. They are calculated on the basis of Eqs. (26), (27)¹⁰⁾ in the scenarios with free and in-medium $P_c^+(4312)$, $P_c^+(4440)$ and $P_c^+(4457)$ spectral functions for branching ratios $Br[P_{ci}^+ \rightarrow J/\psi p] = 1\%$. It is seen that the resonance formation is smeared out by Fermi motion of intranuclear protons. It is a considerably enhanced for the in-medium case at all photon energies of interest. One can also see that at subthreshold incident energies ($E_\gamma < 8.2$ GeV) the main contribution to the J/ψ production on nuclei will come from the intermediate $P_c^+(4312)$ state, while at above threshold beam energies ($E_\gamma > 8.2$ GeV) the resonances $P_c^+(4440)$ and $P_c^+(4457)$ will dominate in this production.

Excitation functions for non-resonant production of J/ψ mesons as well as for their resonant production via $P_c^+(4312)$, $P_c^+(4440)$ and $P_c^+(4457)$ resonances formation and decay in γC and γPb reactions are given in Figs. (5) and (6), respectively. The former ones are calculated using Eq. (4) for five adopted options for the J/ψ in-medium mass shift, whereas the latter ones are determined using Eqs. (26), (27) in the in-medium $P_c^+(4312)$, $P_c^+(4440)$ and $P_c^+(4457)$ spectral functions scenario and

¹⁰⁾By assuming that in Eq. (27) $Br[P_{ci}^+ \rightarrow J/\psi p] = 1$ for all i considered.

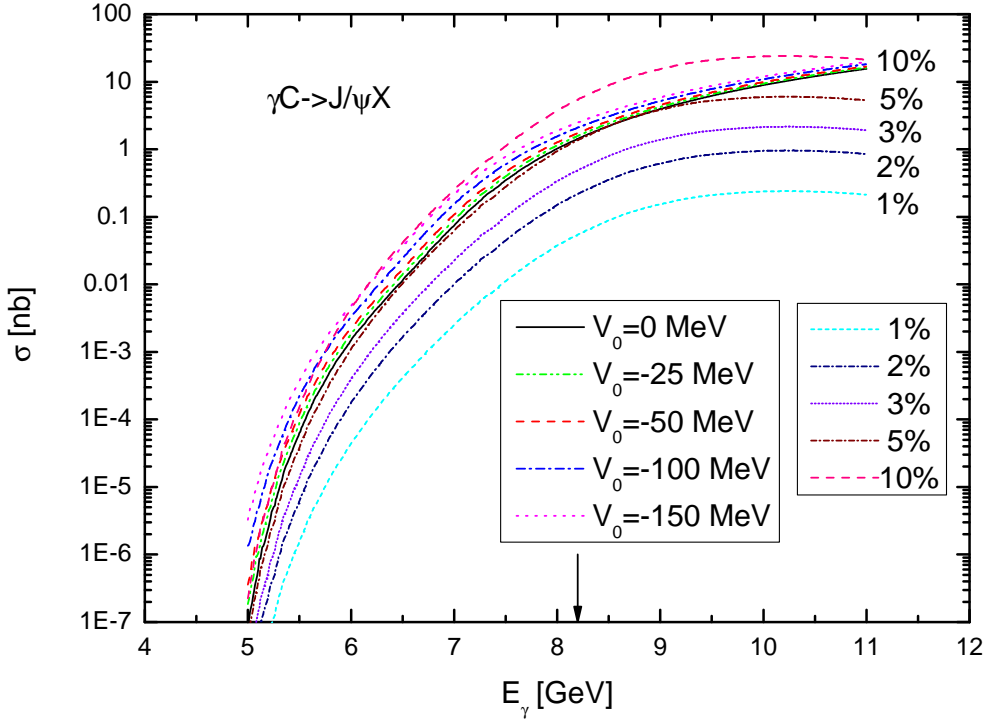


Figure 5: (color online) Excitation functions for the non-resonant and resonant production of J/ψ mesons off ^{12}C from direct $\gamma N \rightarrow J/\psi N$ and resonant $\gamma p \rightarrow P_c^+(4312) \rightarrow J/\psi p$, $\gamma p \rightarrow P_c^+(4440) \rightarrow J/\psi p$ and $\gamma p \rightarrow P_c^+(4457) \rightarrow J/\psi p$ reactions going on an off-shell target nucleons. The curves, corresponding to the non-resonant production of J/ψ mesons, are calculations with an in-medium J/ψ mass shift depicted in the inset. The curves, belonging to their resonant production, are calculations for three branching ratios $Br[P_{ci}^+ \rightarrow J/\psi p] = 1, 2, 3, 5$ and 10% adopting in-medium P_{ci}^+ spectral functions. The arrow indicates the threshold energy for direct J/ψ photoproduction on a free target nucleon being at rest.

assuming that all three branching ratios $Br[P_{ci}^+ \rightarrow J/\psi p] = 1, 2, 3, 5$ and 10% . It can be seen that in the subthreshold energy region ($E_\gamma \sim 5\text{--}8$ GeV) the influence of the J/ψ meson mass shift on its non-resonant yield is significant. Moreover, this influence is not masked by the resonantly produced J/ψ mesons due to the smallness here of their production cross sections compared to the non-resonant ones, if all $Br[P_{ci}^+ \rightarrow J/\psi p]$ are less than 5% . In this case, the differences between the options $V_0 = 0$ MeV, $V_0 = -50$ MeV, $V_0 = -100$ MeV and $V_0 = -150$ MeV for J/ψ in-medium mass shift can be experimentally distinguishable for both considered target nuclei ¹¹⁾. Thus, for incident photon energy of 5 GeV the J/ψ non-resonant yield is enhanced at mass shift $V_0 = -50$ MeV by about a factor of 4.0 as compared to that obtained without this shift. When going from $V_0 = -50$ MeV to $V_0 = -100$ MeV and from $V_0 = -100$ MeV to $V_0 = -150$ MeV the enhancement factors are about 3.5 and 2.5, respectively. At initial beam energy of 8 GeV these enhancement factors are smaller and are about 1.3, 1.3 and 1.25. However, the J/ψ production cross sections at energy of 5 GeV are less than those at beam energy of 8 GeV by several orders of magnitude. This makes the excitation function measurements of J/ψ production at far subthreshold photon energies (at $E_\gamma \sim 5\text{--}6$ GeV) a real challenge due to low cross sections here. But at beam energies not far below

¹¹⁾The small mass shifts ($V_0 \sim -25$ MeV) will probably be experimentally inaccessible.

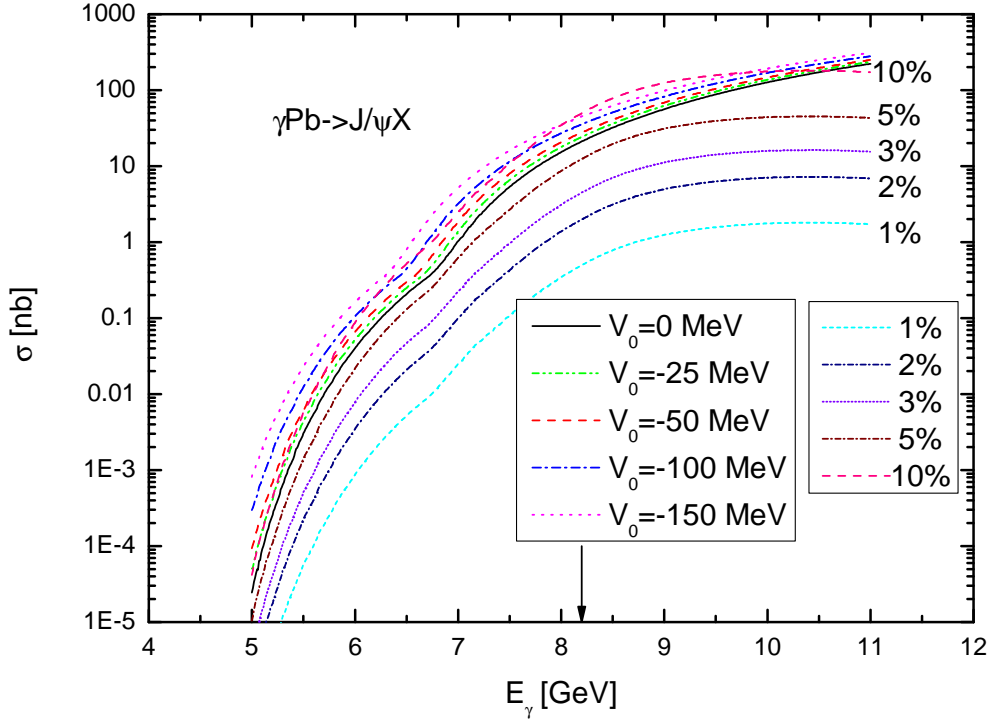


Figure 6: (color online) The same as in figure 5, but for the ^{208}Pb target nucleus.

the threshold (at $E_\gamma \sim 7\text{--}8$ GeV), the charmonium non-resonant production cross sections have a measurable strength $\sim 0.1\text{--}40$ nb. Therefore, the measurements of J/ψ excitation functions in γA reactions in the energy region not far below the threshold with the aim of distinguishing at least between zero, weak ($V_0 \sim -50$ MeV), relatively weak ($V_0 \sim -100$ MeV) and strong ($V_0 \sim -150$ MeV) J/ψ mass shifts in nuclear matter look promising, if three branching ratios $Br[P_{ci}^+ \rightarrow J/\psi p]$ are less than 5%. At above threshold photon energies of 8.2–11.0 GeV the influence of the J/ψ meson mass shift on its non-resonant yield is insignificant. Therefore, it cannot mask the contribution from the resonantly produced J/ψ mesons. Here, the non-resonant J/ψ yield (for considered options for the mass shift) and that from the production and decay of the intermediate $P_c^+(4312)$, $P_c^+(4440)$ and $P_c^+(4457)$ resonances are comparable for all $Br[P_{ci}^+ \rightarrow J/\psi p] \sim 5\text{--}10\%$. If all $Br[P_{ci}^+ \rightarrow J/\psi p]$ are less than 5%, then the former yield is substantially larger, as at subthreshold energies, than the corresponding resonant one. This means that the combined (non-resonant plus resonant) total cross sections for J/ψ production on target nuclei of interest will be enhanced compared to non-resonant ones above threshold for all $Br[P_{ci}^+ \rightarrow J/\psi p] \sim 5\text{--}10\%$ and will not be practically influenced here by the J/ψ in-medium mass shift. Thus, if $Br[P_{ci}^+ \rightarrow J/\psi p] \sim 5\%$ and more, the presence of three P_{ci}^+ resonances in J/ψ photoproduction, on the one hand, leads to additional enhancements in the behavior of the total J/ψ production cross section on nuclei above threshold, which could be studied at JLab to get further evidence for their existence. On the other hand, such presence can mask the modification of the mass of the non-resonantly photoproduced J/ψ mesons in nuclear matter and, therefore, makes the determination of this modification from the excitation function measurements at subthreshold incident energies ($E_\gamma \sim 7\text{--}8$ GeV) difficult.

Therefore, taking into account the above considerations, one can conclude that the J/ψ excitation function measurements at incident photon energies below the production threshold on the free target nucleon will allow to get a deeper insight into the possible J/ψ in-medium mass shifts in the

range of -50 MeV and more only if three branching ratios $Br[P_{ci}^+ \rightarrow J/\psi p]$ are less than 5%¹²⁾. It is valuable to remind that upper limits on these ratios, found by the GlueX Collaboration [4], are within this range.

4. Conclusions

In this work we have calculated the absolute excitation functions for the non-resonant and resonant photoproduction of J/ψ mesons off ^{12}C and ^{208}Pb target nuclei in the near-threshold beam energy region of 5–11 GeV by considering incoherent direct ($\gamma N \rightarrow J/\psi N$) and two-step ($\gamma p \rightarrow P_c^+(4312)$, $P_c^+(4312) \rightarrow J/\psi p$; $\gamma p \rightarrow P_c^+(4440)$, $P_c^+(4440) \rightarrow J/\psi p$; $\gamma p \rightarrow P_c^+(4457)$, $P_c^+(4457) \rightarrow J/\psi p$) J/ψ production processes within a nuclear spectral function approach. It was demonstrated that the non-resonant subthreshold J/ψ photoproduction on nuclei reveals well sensitivity to the possible J/ψ in-medium mass shifts in the range of -50 MeV and more, which is not masked by the resonantly produced J/ψ mesons, only if three branching ratios $Br[P_c^+(4312) \rightarrow J/\psi p]$, $Br[P_c^+(4440) \rightarrow J/\psi p]$ and $Br[P_c^+(4457) \rightarrow J/\psi p]$ are less than 5%. It was also shown that if these branching ratios more than 5% then the presence of the $P_c^+(4312)$, $P_c^+(4440)$ and $P_c^+(4457)$ resonances in J/ψ photoproduction produces above threshold additional enhancements in the behavior of the total J/ψ creation cross section on nuclei, which could be also studied in the dedicated experiment at the CEBAF facility to provide both further evidence for their existence and valuable information on their nature.

References

- [1] E. Ya. Paryev and Yu.T. Kiselev, Nucl. Phys. A **978**, 201 (2018); arXiv:1810.01715 [nucl-th].
- [2] R. Aaij *et al.* (LHCb Collaboration), Phys. Rev. Lett. **115**, 072001 (2015); arXiv:1507.03414 [hep-ex].
- [3] R. Aaij *et al.* (LHCb Collaboration), Phys. Rev. Lett. **122**, 222001 (2019); arXiv:1904.03947 [hep-ex].
- [4] A. Ali *et al.* (The GlueX Collaboration), Phys. Rev. Lett. **123**, 072001 (2019); arXiv:1905.10811 [nucl-ex].
- [5] X.-Y. Wang, X.-R. Chen, and J. He, Phys. Rev. D **99**, 114007 (2019).
- [6] D. Winney *et al.*, Phys. Rev. D **100**, 034019 (2019); arXiv:1907.09393 [hep-ph].
- [7] S. J. Brodsky, E. Chudakov, P. Hoyer, J. M. Laget, Phys. Lett. B **498**, 23 (2001).
- [8] B. Gittelman *et al.*, Phys. Rev. Lett. **35**, 1616 (1975).
- [9] V. Kubarovsky and M. B. Voloshin, Phys. Rev. D **92**, 031502 (2015); arXiv:1508.00888 [hep-ph].

¹²⁾It should be pointed out again that in Ref. [1] the role of initially claimed by the LHCb Collaboration pentaquark resonance $P_c^+(4450)$, having the quantum numbers $J^P = (5/2)^+$, in J/ψ photoproduction on nuclei near threshold was found to be insignificant only if $Br[P_c^+(4450) \rightarrow J/\psi p] \sim 1\%$ and less.

- [10] X.-Y. Wang *et al.*, Phys. Lett. B **797**, 134862 (2019);
arXiv:1906.04044 [hep-ph].
- [11] M. Karliner and J. L. Rosner, Phys. Lett. B **752**, 329 (2016).
- [12] K. A. Olive *et al.* (Particle Data Group), Chin. Phys. C **38**, 090001 (2014).
- [13] C.-J. Xiao *et al.*, Phys. Rev. D **100**, 014022 (2019).
- [14] A. Ali *et al.*, arXiv:1907.06507 [hep-ph].
- [15] H. X. Chen, W. Chen and S.-L. Zhu, Phys. Rev. D **100**, 051501 (2019);
arXiv:1903.11001 [hep-ph].
- [16] R. Chen, Z. F. Sun, X. Liu and S.-L. Zhu, Phys. Rev. D **100**, 011502 (2019);
arXiv:1903.11013 [hep-ph].
- [17] F. K. Guo, H. J. Jing, U. G. Meissner and S. Sakai, Phys. Rev. D **99**, 091501 (2019);
arXiv:1903.11503 [hep-ph].
- [18] M. Z. Liu *et al.*, Phys. Rev. Lett. **122**, 242001 (2019);
arXiv:1903.11560 [hep-ph].
- [19] J. R. Zhang, arXiv:1904.10711 [hep-ph].
- [20] H. Huang, J. He and J. Ping, arXiv:1904.00221 [hep-ph].
- [21] Y. Shimizu, Y. Yamaguchi and M. Harada, arXiv:1904.00587 [hep-ph].
- [22] C. W. Xiao, J. Nieves and E. Oset, Phys. Rev. D **100**, 014021 (2019);
arXiv:1904.01296 [hep-ph].
- [23] L. Meng, B. Wang, G. J. Wang and S.-L. Zhu, Phys. Rev. D **100**, 014031 (2019);
arXiv:1905.04113 [hep-ph].
- [24] J. B. Cheng and Y. R. Liu, Phys. Rev. D **100**, 054002 (2019);
arXiv:1905.08605 [hep-ph].
- [25] A. N. Hiller Blin *et al.*, Phys. Rev. D **94**, 034002 (2016).
- [26] J. Zarling, arXiv:1911.11239 [nucl-ex].